Water and energy fluxes from a woodland savanna (cerrado) in southeast Brazil

Osvaldo M.R. Cabral [a,*], Humberto R. da Rocha [b], John H. Gash [c],
Helber C. Freitas [b], Marcos A.V. Ligo [a]

[a] Embrapa Meio Ambiente, CEP 13820-000, Jaguariúna, SP, Brazil
[b] Universidade de São Paulo, São Paulo, Brazil
[c] Centre for Ecology and Hydrology, Wallingford OX10 8BB, United Kingdom

ARTICLE INFO

ABSTRACT

Study region: The area of woodland savanna (cerrado) is located in southeast Brazil (21°36′ to 44′ S, 47°34′ to 41′ W).

Study focus: The cerrado *sensu-stricto* savanna evapotranspiration was observed using the eddy-covariance method over three years.

New hydrological insights for the region: The first year total rainfall (R = 1664 mm) was 11% above the long-term rainfall (1498 mm) and the total evapotranspiration (ET = 1242 mm) and water equivalent of available energy (A_v = 1835 mm) were approximately 4% and 2% greater, respectively, than in the second year when the rainfall total was 5% lower than the long-term average. In the third year despite the total rainfall (1259 mm) being 24% lower than the first year and 16% lower than the average, the totals of ET (1242 mm) and A_v (1815 mm) were approximately the same.

The small variation in the observed annual ET totals shows that in this cerrado vegetation the deep soil moisture content supports the ET in a dry year and the water available for recharging the soil profile and groundwater ($\sim R$ − ET) was dominated by the rainfall amount being significantly greater in the wet year (422 mm) than in the dry year (13 mm).

© 2015 The Authors. Published by Elsevier B.V. This is an open access article under the CC BY-NC-ND license (http://creativecommons.org/licenses/by-nc-nd/4.0/).

* Corresponding author. Tel.: +55 19 33112685; fax: +55 19 33112640.
E-mail addresses: osvaldo.cabral@embrapa.br, osvaldomrcabral@gmail.com (O.M.R. Cabral).

1. Introduction

The savanna, or cerrado, of Brazil is one of the most threatened biomes in the tropics (Marris, 2005). Originally covering about 23% of Brazil, almost 2 million km^2, it now covers just 20% of that original area (Goulart et al., 2005). Land-use change in the cerrado is a relatively recent process, with more than 50% having been transformed into pasture and arable agricultural land over the last 40 years (Klink and Machado, 2005). Protected reserves amount to only approximately 2% of the original area, despite the richness of its biodiversity (∼10,000 plant species; Myers et al., 2000). Indeed, based on recent trends in deforestation (Bianchi and Haig, 2013), cerrado may effectively no longer exist in 25 years time. Cerrado exhibits a gradient (Bustamante and Ferreira, 2011) ranging from grassland to sclerophyllous forest (cerradão), with intermediate physiognomies characterized by an increasing density of woody species (campo sujo, campo cerrado, and cerrado *sensu-stricto*, see Ruggiero et al., 2002). The fragmentation typifies the spatial heterogeneity as found by Silva et al. (2006), whose results showed a patchy physiognomy of native vegetation even at a local scale.

The climate of the vast cerrado region (approximately from 10° S to 23° S latitude, see Bustamante and Ferreira, 2011; Vourlitis and da Rocha, 2011) is characterized by mean annual temperatures ranging from 26 °C in the north to 20 °C in the south; the annual rainfall varies from 2000 mm in the north to 1200 mm in the south and is highly seasonal, with more than 80% occurring in the Southern Hemisphere summer (the rainy-season, October to April) and with marked inter-annual variability (Batlle-Bayer et al., 2010). Many species have deep root systems, for example Ferreira et al. (2007) observed water depletion by plants down to 10 m depth, which allow transpiration to be maintained even during the dry months (the dry-season, May to August) as reported by Oliveira et al. (2005). Thus, the current replacement of the native vegetation by shallow-rooted crops and pasture could potentially alter the regional hydrology (Oliveira et al., 2005; Silva et al., 2006). As a first step towards estimating the impacts of cerrado land-use change on the hydrological cycle, our objective here is to quantify the surface energy and water balances for one the main types of cerrado (Miranda et al., 1997; Giambelluca et al., 2009; Lorz et al., 2012).

To measure the energy exchange and latent heat flux in a landscape with such high spatial heterogeneity requires a technique capable of sampling at a scale comparable with, or exceeding, the scale of variability of the ecosystem. The eddy-covariance technique (Aubinet et al., 2000; Baldocchi et al., 2001; Kirschbaum et al., 2007) is the most suitable method because it samples water vapor fluxes with a measurement footprint of several hectares upwind (Schmid, 1997).

We applied the eddy-covariance technique over three years to measure the water and sensible heat fluxes from a remnant of cerrado savanna in the southeast of Brazil. The main objectives were to determine the seasonal controls of climate (net all-wave radiation, air humidity and soil moisture) on the cerrado evapotranspiration and energy partition, as well as the effects on the surface bulk parameters, i.e., the canopy conductance. Water is a scarce resource in this region and the substitution of cerrado by grasses, crops and forest plantations may affect the dynamics of the regional atmosphere (cloudiness, humidity, surface temperature) and promote changes in runoff and in the duration of the dry season as reviewed by Rodrigues et al. (2014). The quantification of seasonal variations in the energy fluxes and the identification of the environmental controls of evapotranspiration for the mosaic of cerrado physiognomies (Santos et al., 2003; Hoffmann et al., 2005; Oliveira et al., 2005; Giambelluca et al., 2009; Biudes et al., 2015) will help us to understand the role of cerrado vegetation in the regional hydrological cycle.

2. Methods

2.1. Site

The study was conducted in the reserve Pé de Gigante (PdG): an area of 1213 ha of cerrado vegetation (21°36′ to 44′ S, 47°34′ to 41′ W, altitude from 590 to 740 m), in the Vassununga State Park (Instituto Florestal) in São Paulo State, Brazil (Batalha et al., 2001; da Rocha et al., 2002). The reserve contains natural vegetation, but is surrounded by eucalyptus and sugarcane plantations (see Cabral et al., 2010, 2012). From the Quesada et al. (2004) physiognomy descriptions and the Batalha and
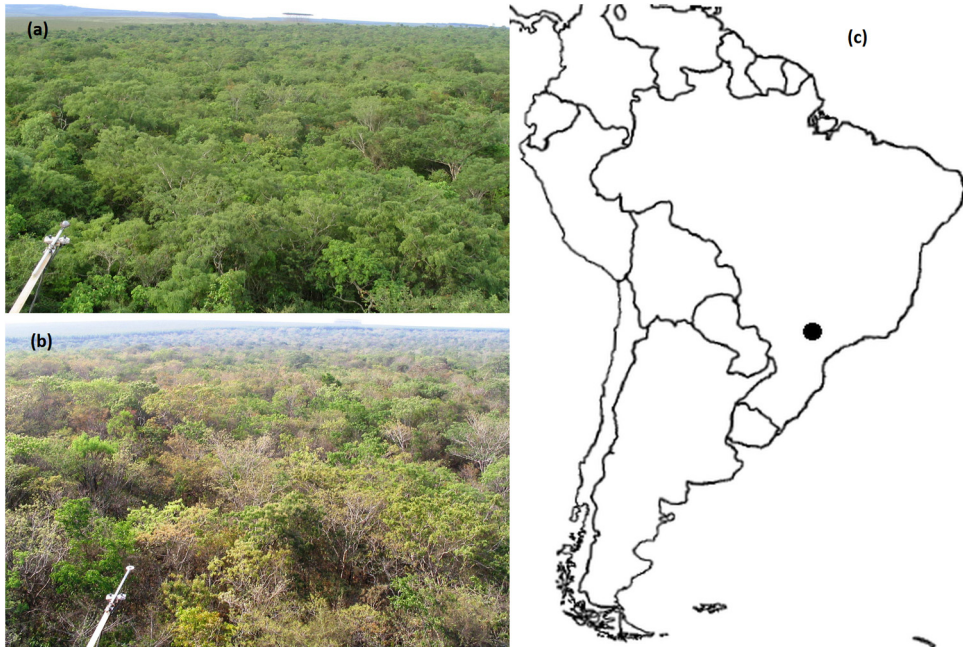
Fig. 1. Photographs of the Pé de Gigante cerrado vegetation (mean canopy height 5 m) seen from the scaffolding tower (21 m) in (a) the wet-January and (b) dry-September seasons. (c) Map showing the region of the cerrado area (black circle).

Mantovani (2001) vegetation survey the reserve composition is given as: 79% cerrado *sensu-stricto* (closed scrub with tall trees, a dense woody undergrowth, and grasses); 11% cerradão (closed-canopy forest with dense woody undergrowth and sparse grasses); 8% campo cerrado (open scrub formed by a denser woody layer and grasses) and <1% campo sujo (open savanna with scattered small trees and shrubs over a continuous herbaceous layer). Photographs of the vegetation seen from the solar radiation measurement tower (see Section 2.2 below) are shown as Fig. 1 during the wet (January) and dry (September) seasons.

The importance of the cerrado in terms of land use and vegetation types can be assessed from the aerial photographic survey done in the year 1962 (Borgonovi and Chiarini, 1965; Borgonovi et al., 1967) in São Paulo State (248,600 km^2). The area of natural vegetation was 7,257,400 ha (29% of the State) and 3,851,500 ha in the cerrado physiognomies (or 15.5%) and 2,668,000 ha (37%) of cerrado *sensu-stricto*. In 2001 the natural vegetation area was 3,457,301 ha and the area of cerrado was reduced to 140,493 ha (SEMA, 2005).

The area around the tower is cerrado *sensu-stricto* (da Rocha et al., 2002, 2009). According to the forest inventories conducted in PdG by Batalha et al. (2001) and Fidelis and Godoy (2003) approximately 70% of the individuals (17,175 ± 3719 ha^{-1}) had stem diameters <5.5 cm and the height of 85% of the trees was <5 m, without any well-defined canopy strata. The survey of the patchy understory vegetation recorded 159,600 ± 42,350 individuals ha^{-1}, from 81 species in the herbaceous component of the PdG site at the end of the rainy season (Batalha et al., 2001). However there is a mosaic of species which exhibit different leaf phenologies (see Williams et al., 1997) as the evergreen (full canopy throughout the year), semideciduous (canopy falls to below 50% of full canopy in the dry season) and brevi-deciduous species (canopy falls significantly, but briefly). The leaf area index (LAI) ranged from 3.0 to 0.7 (m^2 leaf m^{-2} ground) in the rainy and dry seasons, respectively; based on estimates derived from hemispherical photographs (Frazer et al., 2001) calibrated against the total yearly leaf litter fall (see Roberts et al., 1993), collected on a monthly basis (32 trays of 0.25 m^2) and allowing for biomass decay of 3% (see Valenti et al., 2008). The mean specific leaf litter area (SLA = 6.78 ± 0.08 m^2 kg^{-1}) was obtained from the dry weight and areas of sub-samples (10% of the total).

The soil is quartz sand (Typic Quartzipsamment); the mean fractions are 87% sand; 3% silt and 10% clay. The average dry bulk density and standard deviation in the 2 m layer is 1552 ± 127 kg m^{-3}, and the available soil water defined as the soil water content between the matric potentials of -33 and -1500 kPa is 81 mm m^{-1} depth. Although the extent of the root system was not determined we observed roots down to 2 m depth during the soil sampling. This depth agrees with the results obtained in other cerrado sites where deep root systems were also found (Canadell et al., 1996; Oliveira et al., 2005; Giambelluca et al., 2009).

The regional mean annual precipitation (30-year) and standard deviation is 1498 ± 312 mm with the minimum observed in the dry-season (June, 32 mm) and the maximum in the rainy-season (January, 266 mm). The annual average of the mean daily air temperature is 22.1 ± 0.5 °C, varying between 19 and 24 °C.

2.2. Instrumentation

The data presented here were collected on two separate micromet towers. The sensible heat (H) and water vapor fluxes (LE) were measured at the top of a 11.4 m triangular lattice mast of 0.3 m cross section using a three-dimensional sonic anemometer (CSAT3, Campbell SI, Logan, UT, USA) and an open-path infrared gas analyzer (IRGA, LI7500, Li-Cor, Lincoln, NE, USA). Approximately 100 m to the southeast (21°37′16.1″ S, 47°38′2.0″ W; altitude 705 m), was a second 21 m high scaffolding tower; this tower was previously used by da Rocha et al. (2002, 2009). We installed a 2.5 m horizontal mast at 18 m height from which we measured: net radiation (R_n, LITE, Kipp and Zonen, Delft, The Netherlands), the incident and reflected fluxes of photosynthetically active radiation (PAR, LITE, Kipp and Zonen), and global solar radiation (R_g, CM3, Kipp and Zonen). The rainfall (TB4, Hydrological Services Pty. Ltd., NSW, Australia), and air temperature and humidity (HMP45 Vaisala, Helsinki, Finland) were measured at 21 m height.

Soil heat flux (G) was measured as the mean of four plates (REBS, Seattle, WA, USA) randomly installed at 2 cm depth and the soil water content (SWC) was measured by reflectometers (CS615, Campbell SI) installed horizontally in a trench at the following depths: 0.1; 0.2; 0.5; 0.8; 1.0; 1.5; 2.0 and 2.5 m. All the data (10 min averages or totals) were recorded on flash cards by two dataloggers (CR1000, Campbell SI).

2.3. Data processing

Eddy-covariance fluxes were calculated from the 20 Hz fluctuations around 30-min block averages which were then corrected for the effects of density (Webb et al., 1980) and self-heating of the IRGA windows (Burba et al., 2008); the mean vertical wind speed (w) was forced to be zero by a double coordinate rotation (Kaimal and Finnigan, 1994). The high frequency spectral correction was based on the in situ determination of the system cut-off frequency (see Ibrom et al., 2007), and the corrections to account for sonic wind distortions and vertical separations (sonic and Irga) were based on Horst and Lenschow (2009) as implemented in the EddyPro5 software (Li-Cor, Lincoln, NE, USA).

The storage flux (S_a) due to the changes in the sensible and latent heat content of the canopy air beneath the eddy-covariance measurement height was estimated from the time variation of air temperature and humidity above the canopy (Aston, 1985; Moore and Fisch, 1986; Michiles and Gielow, 2008; Giambelluca et al., 2009; Cabral et al., 2010). The biomass energy storage (S_b) was derived from bark temperature measured with thermocouples installed at breast height in four trees whose diameter at breast height (dbh) spanned the range of the inventory distribution (6.7; 6.9; 10.5 and 14.9 cm). In one tree (dbh = 14.9 cm) thermocouples were installed at three different heights (1.3; 3.7 and 5.8 m) to sample the vertical variation (Silberstein et al., 2001). The specific heat of the moist wood biomass (Moore and Fisch, 1986; Michiles and Gielow, 2008) was calculated from the average cylindrical volume (164.79 ± 62.50 m^3 ha^{-1}, Batalha et al., 2001; Fidelis and Godoy, 2003); wood density (0.63 ± 0.18 g cm^{-3}, mean of 60 species given by Quirino et al., 2005) and the wood moisture content (49%) estimated from the ratio between dry and fresh average biomass given by Rezende et al. (2006). We assumed the branch biomass was already included in the given overestimated cylindrical volume and the leaf biomass was obtained from the time series of LAI and the mean SLA. The available energy

(A_v) providing the latent (LE) and sensible heat (H) fluxes was calculated as $A_v = R_n - G + S_a + S_b$, where the rate of energy consumption in photosynthesis was assumed to be negligible (Oliphant et al., 2004).

We have calculated the canopy conductance to water vapor fluxes (g_c) based on the inverted Penman–Monteith equation (Monteith, 1965) and the aerodynamic conductance (g_a) from the friction velocity and horizontal wind (Gash et al., 1999). The coupling between the vegetation and the atmospheric boundary layer above was assessed by the omega (Ω) factor (McNaughton and Jarvis, 1983).

2.3.1. Gap filling

Missing latent heat fluxes (LE) amounted to 20% of the total number of possible 30-min data points (52,560) during the three years of observations. Rainfall wetting the IRGA windows was the most common cause of missing data, although in February 2010 a power failure shut down the eddy-covariance system for 15 days. However the temporal data coverage obtained was similar to the 21% reported for other sites (Falge et al., 2001).

Based on the energy balance closure results (see Section 3.1) the missing LE data were estimated as the residuals (LE = $A_v - H$) when the sensible heat fluxes (H) were available; if not, then the small gaps (<1 day) were filled by the mean diurnal variation (Falge et al., 2001) calculated over a 15-day moving window and for longer gaps (>1 day) from the relationships between LE and R_n, fitted over variable time windows. We have also used the data from the closest weather station approximately 18 km distant (São Simão-CIIAGRO, 21°29′ S, 47°33′ W, and 667 m altitude) after inter-comparison to fill the gaps in the other environmental variables.

The results of the model Hydrus1D (Šimůnek et al., 2008) were used to gap-fill the missing soil moisture data. The upper boundary condition was given by the measured rainfall and evapotranspiration with surface runoff and free drainage as the lower boundary condition (3.5 m depth). The hydraulic model of van Genuchten–Mualen (no hysteresis) was used for the sandy soil ($\theta_r = 0.045$; $\theta_s = 0.430$; $\alpha = 0.240$ cm^{-1}; $n = 2.08$; $K_s = 713$ cm day^{-1}; $l = 0.5$), and the main processes simulated were water flow and root water uptake (S shape model; $P_{50} = -1000$; $P_3 = 3$ and no solute stress) in a 2 m depth soil profile with the root distribution decreasing linearly with depth.

2.4. Rainfall interception modeling

The rainfall interception loss (I) was estimated applying the revised Gash model (Gash et al., 1995). The canopy cover parameter ($c = 1$ closed canopy) was estimated as 0.72 based on the analysis of hemispherical photographs (GLA software; Frazer et al., 2001) recorded in summer at the PdG site. The intercepts of regressions (Lloyd et al., 1988) between throughfall and stemflow versus gross rainfall obtained by San Jose and Montes (1992) in the Orinoco Llanos savanna provided the estimated mean stores for canopy ($S_c = 0.73 \pm 0.14$ mm) and stem ($S_t = 0.04 \pm 0.02$ mm); from the slopes reported for trees with diameters <0.2 m by San Jose and Montes (1992) the stemflow partitioning coefficient (p_t) was estimated as 0.019 (see Valente et al., 1997).

The mean hourly evaporation from the wet canopy, where it is present ($\bar{E}_c = 0.08$ mm h^{-1}), was obtained from the measured canopy cover and the residual in the energy balance equation based on the sonic anemometer data (see Cabral et al., 2010) and another net radiometer, the Q*7.1 (REBS, Seattle, WA, USA) which was operational during 577 rainy periods of 30 min totaling 1083 mm, and covering the dry and wet periods of the year. Although not entirely free of errors during rainfall the Q*7.1 performance is better than the LITE instrument (see Brotzge and Duchon, 2000). According to Czikowsky and Fitzjarrald (2009) in rainy conditions the typical decrease in the net radiation signal (25 W m^{-2}) lowers the evaporation between 2 and 5%. For this same period of time the mean hourly rainfall rate ($\bar{R}$) was 3.7 mm h^{-1} (see Wallace and McJannet, 2008).

3. Results and discussion

3.1. The flux footprint and energy balance closure

The fetch of cerrado *sensu-stricto* around the flux tower was greater than 500 m in all directions. At 200 m in the southeasterly direction there is a pronounced slope, however the wind frequency from

this sector accounted for approximately only 10% of the daylight hours during the summer; it therefore represents a relatively small contribution. The mean peak distance (X_p; see Hsieh et al., 2000) from the measuring point to the maximum contributing source area was 40 ± 11 m for daylight hours and 60 ± 15 m overnight; the fetch-to-height ratio to recover 90% of the fluxes varied from 120 to 140 overnight and was less than 100 during unstable daytime conditions.

The energy balance closure (see Wilson et al., 2001; Culf et al., 2004; Leuning et al., 2005; Foken, 2008) is shown in Fig. 2a. The measurement height was approximately twice the canopy height. Measurements were thus made in the roughness sub-layer where high frequency flux loss may be common because the flow characteristics are strongly influenced by tree elements (Su et al., 2004). The ensemble averaged normalized cospectra obtained over 30 days in the wet (March) and dry (August) seasons for unstable conditions (Fig. 2b and c) were more peaked than in the surface layer over flat terrain (Kaimal and Finnigan, 1994; Sakai et al., 2001) however the attenuation of the sensible heat fluxes (wt) was less than 3% while for the latent heat fluxes (wq) the attenuation was about 3–4% during the daytime and 6–10% at night on average.

The slope (1.0, $R^2 = 0.95$) of the linear regression of the sum of turbulent fluxes of heat and water vapor, against the available energy (Fig. 2a) indicates that the positioning of the new flux tower exhibited an adequate fetch of homogeneous surface (see Baldocchi, 2003) matched as well by the net radiation sensor (see Schmid, 1997; Schmid and Lloyd, 1999), contrasting with the previous data reported by da Rocha et al. (2009) where the closure achieved was 0.7 (included spectral corrections for the closed path IRGA without the energy storage estimates). However the results of Frank et al. (2013) showed that the non-orthogonal sonic anemometer utilized here (CSAT3, Campbell SI) can lead to 10% underestimation in w; if their result is generally applicable this assumption must be reassessed.

3.2. The climate

The data collected covered a three-year period from 2 July 2009 (Day 183) until July 2012. The data are typical of the region's climate: with hot, humid rainy-seasons and cool dry-seasons with low humidity. The daily mean air temperatures in the rainy-season achieved 27 °C (Fig. 3a), at the same time mean water vapor saturation deficits (D) as small as 0.1 kPa were recorded. During the mild dry-season occasionally mean air temperatures as low as 12 °C were measured; these were associated with the passage of cold fronts with drier air, as can be seen from the larger mean saturation deficits (3 kPa).

The total rainfall (Fig. 3b) observed during the first year (1664 mm; from July 2009 to July 2010) was 11% above the long-term average (1498 ± 312 mm), and in the second year (1422 mm) was 5% lower than the average, however in the third year the total rainfall (1259 mm) was 24% lower than the first year and 16% lower than the average.

The greater total rainfall observed in the first year mainly resulted from the anomalously wet dry-season during July–August–September 2009, when the cumulative rainfall was 356 mm. In 2010 and 2011 the observed totals over the same period were 70 mm and 53 mm, respectively, while in the third year resulted from the lower amount of rainfall received in wet season (391 mm; from January to March), than in the previous years (540 and 671 mm, respectively) – characteristic of the inter-annual variability (see Dufek and Ambrizzi, 2008; Marengo and Camargo, 2008). Notice the humidity saturation deficits (Fig. 3a) were also lower due to the more frequent rainfall in the winter of 2009. The PAR reflection coefficient (r_{PAR}; Fig. 3c) calculated as the 15-day moving-average ratio of reflected over the incident daily PAR totals followed the seasonal variation in soil moisture content (2 m depth layer), and the highest r_{PAR} occurred when the lowest level of soil moisture was achieved in August 2011 (89 mm).

We notice in Fig. 3c the beginning of a new flush of vegetative growth in September 2010 and 2011 prior to the onset of the rainy-season as well as the expected lower values in the dry-season (Lenza and Klink, 2006; Lloyd et al., 2009).

The seasonal patterns of LAI obtained from hemispherical pictures calibrated against the total yearly leaf litter fall, followed the inverse of the PAR reflection coefficient (r_{PAR}). This enabled us to establish a functional relationship between LAI and r_{PAR} (LAI = 0.0038 $r_{PAR}^{-1.84}$; $R^2 = 0.992$)–such relationships can
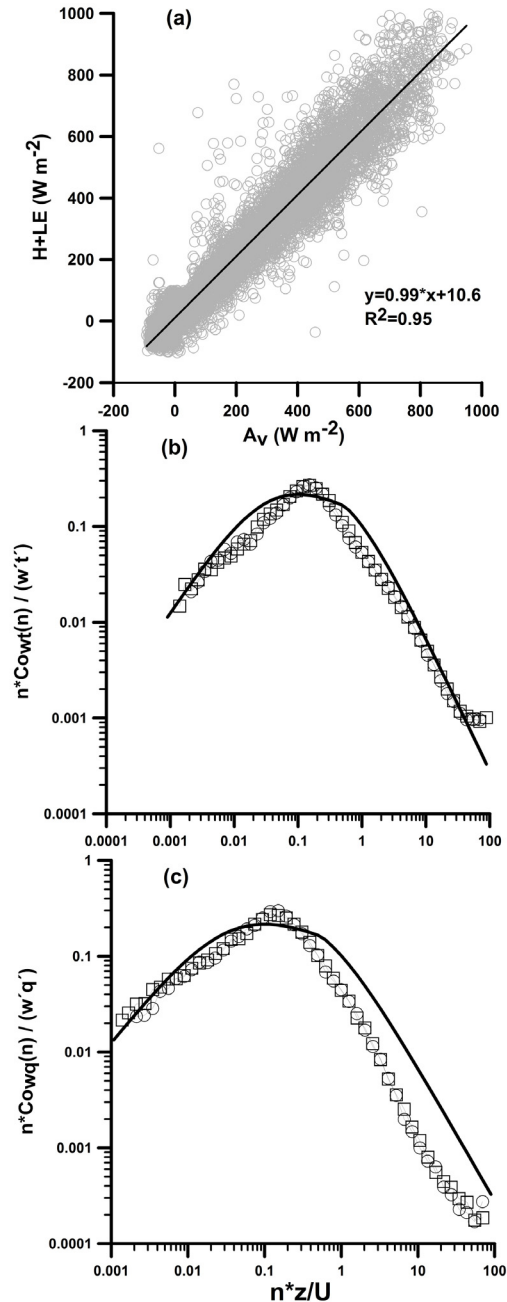
Fig. 2. (a) Scatter plot between the sum of turbulent fluxes (30 min) of sensible (H) and latent heat (LE) versus the available energy ($A_v = R_n - G - S$). Gap-filled data are not included. Ensemble averaged normalized cospectra for (b) sensible (wt) and (c) latent heat fluxes (wq) during unstable conditions in the wet (circles) and dry (squares) seasons; the solid lines represent the Kaimal and Finnigan (1994) universal curves for cospectra. In the horizontal axis n represents the natural frequency, U the mean wind velocity and z the measurement height.
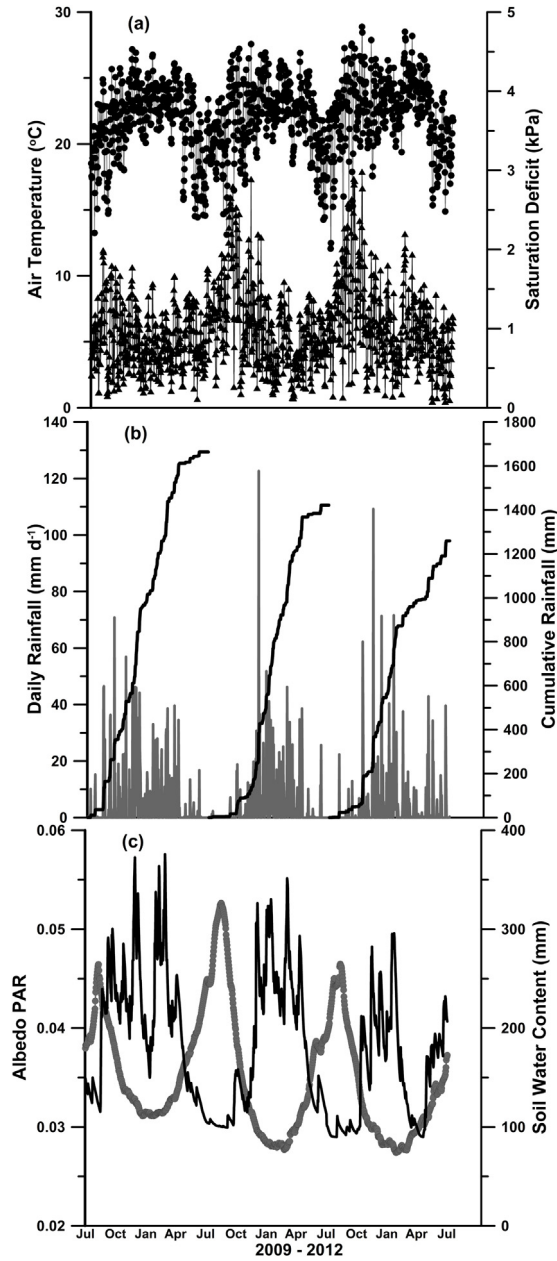
Fig. 3. (a) Daily averages of air temperature (circles) and saturation vapor pressure deficit (triangles); (b) daily total rainfall (gray bars) and the cumulative yearly totals (black line); (c) PAR reflection coefficient (circles) and soil water content (0–2 m layer; black line).
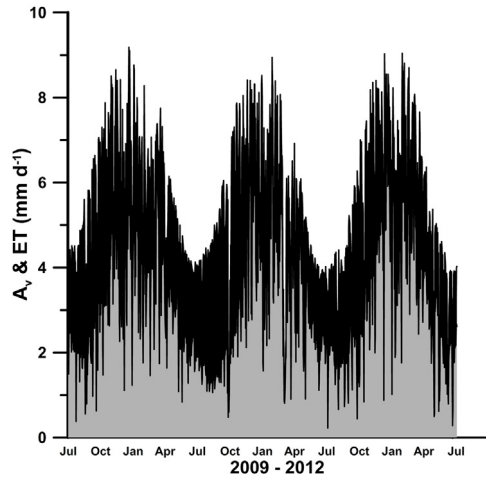
Fig. 4. Daylight totals of available energy (A_v, black bars) and evapotranspiration (ET, gray bars) measured above the cerrado. Units are water equivalent in mm per day.

Table 1
Summary of annual totals of fluxes (water equivalent) of sensible heat (H); evapotranspiration (ET); available energy (A_v); rainfall (R) and interception loss (I).

	H (mm)	ET (mm)	A_v (mm)	R (mm)	I (mm)	ET/A_v	ET/R	$R -$ ET (mm)
Y1[a]	641	1242	1835	1664	120	0.68	0.75	422
Y2[a]	687	1196	1797	1422	116	0.67	0.84	226
Y3[a]	693	1246	1815	1259	91	0.69	0.99	13
Mean	674	1228	1816	1448	109	0.68	0.86	

[a] Y1 is relative to the first year of measurements (183/2009–182/2010); Y2 to the second year (183/2010–182/2011) and Y3 to the third year (183/2011–182/2012).

be useful for modeling and remote sensing (see Hoffmann et al., 2005; Pongratz et al., 2006; da Silva et al., 2014; Rodrigues et al., 2014).

3.3. Observed seasonal patterns

3.3.1. Evapotranspiration and available energy

Daylight totals of the evapotranspiration (ET) and the water equivalent of the available energy (A_v) are displayed in Fig. 4. ET ranged from 1.0 mm day^{-1} in August (dry-season) of 2010 to 7.1 mm day^{-1} in February (summer rainy-season) of 2012 and mostly followed A_v, although the steeper variations in ET from rainy to dry season in each year (46, 63 and 58%, respectively) were greater than the observed decreases in A_v (28, 17 and 34%, respectively) indicating the influence of other factors driving the energy partition such as LAI, soil moisture and D. The highest rates of ET were measured in days following overnight rainfall, as nearly 70% of the rainfall occurred overnight, when A_v increased and the soil litter layer and undergrowth vegetation were wet (see Gash et al., 1991, 1997).

The seasonal variation in ET reported for other cerrado sites (in central Brazil) was somewhat smaller, between 1.5 and 4.6 mm day^{-1} (Oliveira et al., 2005; Quesada et al., 2008; Giambelluca et al., 2009), and lower values of transpiration measured from sap flow (from 0.2 to 0.8 mm day^{-1}) were obtained by Bucci et al. (2008) over different types of cerrado; however, as pointed out by Vourlitis et al. (2008), the sap flow represents only stand-level plants being monitored, while the eddy-covariance derived ET includes the transpiration and evaporation from undergrowth and soil surfaces.

The three annual totals of measured evapotranspiration (Table 1) were 1242, 1196 and 1246 mm yr^{-1}, respectively and the average of evaporative fraction ($\alpha =$ ET/A_v) was 0.68; despite the
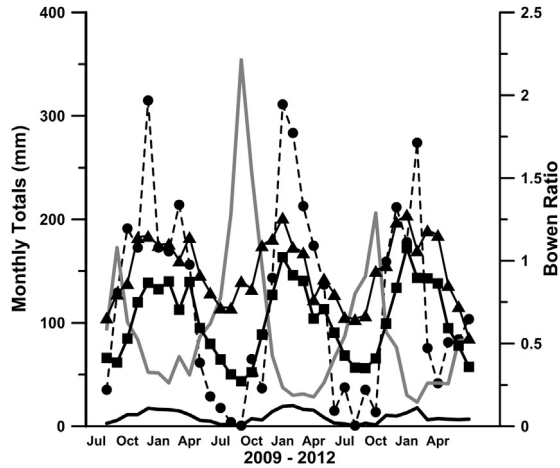
Fig. 5. Monthly totals of rainfall (circles); water equivalent of latent heat flux (squares); available energy (triangles); rainfall interception (black line) and Bowen ratio (gray line).

total rainfall in the first year having been 11% above the average, the total evaporation was approximately 4% greater while in the third year although the total rainfall (1259 mm) being 24% lower than the first year and 16% lower than the average, the total of ET (1242 mm) was approximately the same. The evapotranspiration accounted for 75 and 99% of the total rainfall in each year and on average (1228 mm yr^{-1}) was 82% of the long-term average rainfall (1498 mm yr^{-1}). Therefore in the year with above average rainfall a larger proportion of rainfall was used for soil and groundwater recharge ($\sim R - $ET) because the ET variation between years was smaller (see Zeppel et al., 2008).

Based on the monthly totals (Fig. 5) the evaporative fraction (α) ranged from 0.31 in August 2010 to 0.85 in March 2011. The Bowen ratio ranged from 0.2 in the rainy-season to above 2.0 in the dry-season and exactly followed the seasonal variation in r_{PAR} (Fig. 2c) and therefore LAI, which is almost entirely dependent on the deciduous, semi and brevi-deciduous species (Eamus et al., 2001).

Our results are similar to figures obtained by Quesada et al. (2008) based on the water balance in a cerrado *sensu-stricto* area, where ET accounted for 85% of the rainfall whose totals varied between 1010 and 2443 mm yr^{-1}. Vourlitis et al. (2014) reported an average ET (965 ± 46 mm yr^{-1}) observed in a taller and more dense vegetation area (cerradão) with greater mean annual rainfall (2000 mm) accounting for 46% of the average rainfall (2137 ± 256 mm yr^{-1}) and 57% of the water equivalent mean net radiation (R_n, 1711 ± 54 mm yr^{-1}). The annual total of ET reported by Giambelluca et al. (2009) for a lower tree-density cerrado was 823 mm yr^{-1} and amounted to 71% of the rainfall which was about 20% less than the long-term annual rainfall (1440 mm). These differences mainly result from the cerrado spatial heterogeneity (Silva et al., 2006), enhanced by the distinctive leaf phenology of the species (Williams et al., 1997).

3.3.2. Rainfall interception

The rainfall intercepted by the canopy and lost as evaporation is an important term of the water balance and can represent up to 13% of the rainfall in foliated deciduous forests (see Carlyle-Moses, 2004). The average monthly total rainfall interception (I) was estimated as 16 mm per month from November to February in the first year (Fig. 5), corresponding to approximately 8% of rainfall. The maximum I (20 mm per month) was estimated for January 2011 and accounted for 7% of gross rainfall ($P_g = 284$ mm). The modeled interception losses (I in Table 1) amounted to 7% (120 mm), 8% (116 mm) and 7% (91 mm) of the total rainfall recorded in each year, respectively. Similar results ($I < 10\%$) were observed by Lilienfein and Wilcke (2004) although greater losses ($I > 12\%$) were reported by San Jose and Montes (1992) and $I > 40\%$ of gross rainfall were found in a cerrado *sensu-stricto* site by Quesada et al. (2008). However, interception loss is sensitive to the sparseness of the trees, when

the interception losses are reported on a crown area basis they are greater than when calculated on a ground area basis (David et al., 2006). Also in this case, the results may be valid only for close-to-vertical rainfall events (see David et al., 2006; Pereira et al., 2009). We have obtained a relatively low value for the evaporation of rainfall during storms ($\bar{E}_c = 0.08\,\mathrm{mm\,h^{-1}}$) for the cerrado, mainly because the saturation deficits during rainfall were small ($\sim$0.3 kPa) as most of the rainfall (70%) was observed to occur overnight.

3.3.3. The bulk surface g_c, g_a and Ω

The bulk canopy conductance (g_c, Fig. 6a) exhibited a strong seasonal variation from approximately 20 to 2 mm s^{-1} in rainy and dry seasons, respectively. The decline in g_c results from the stomatal closure and from the seasonal leaf abscission of wood and herbaceous species (Grace et al., 2006). In contrast, the aerodynamic conductance (g_a, in Fig. 6b) exhibited relatively little seasonal variation and the overall average and standard deviation were $129 \pm 59\,\mathrm{mm\,s^{-1}}$.

The decoupling coefficient (Ω, Fig. 6c) ranged from 0.1 in the winter to 0.5 in the summer. Therefore, while the evaporation was mainly regulated by physiological factors and saturation deficits in the dry-season, the intermediate values of Ω observed in the wet-season indicated that the available energy and to some extent the physiology dominated the evaporation (Jarvis, 1985). Based on the limit of $\Omega = 0.5$ adopted by Blanken and Black (2004), this cerrado can be considered as a rough surface with the regional vapor pressure deficits the dominant control on transpiration (Miranda et al., 1997; Bucci et al., 2005); the controls of wind speed and surface roughness on the transpiration rates were secondary.

3.3.4. The mean daily cycles of LE, A_v, D and g_c

The daily cycles of latent heat flux (LE), A_v and g_c are shown in Fig. 7. The hourly averages of both the saturation deficit (D) and LE followed A_v in the morning in both seasons. Average g_c (Fig. 7c) in the rainy-season was approximately four times that in the dry-season, consistent with the observed seasonal decline in soil water content and LAI (from 3.0 to 0.7 m^2 m^{-2}), and the increase in the humidity saturation deficit. In the rainy-season the hourly g_c values moved in parallel to the radiation and vapor pressure deficit (Miranda et al., 1997), but in the dry-season g_c decreased nearly linearly throughout the day (Domec et al., 2006). Other cerrado studies have also reported the rapid early morning increase in g_c and the sharp decline in the afternoon (Meinzer et al., 1999; Goldstein et al., 2008; Giambelluca et al., 2009), but the comparisons are difficult because our results represent the contribution of both deciduous and evergreen species (Meinzer et al., 1999). The g_c values found here are higher than the values reported by Bucci et al. (2008) as well as by Giambelluca et al. (2009), but consistent with their findings that higher g_c were associated with sites showing higher tree density and LAI.

3.4. Environmental controls

The daily totals of ET versus the mean daily saturation deficits (D) are shown in Fig. 8 for wet and dry months. The increase in ET with D in the rainy-season and the nearly constant lower ET observed during the dry-season indicate that the bulk canopy conductance declined towards the dry-season (Eamus et al., 2001; Kutsch et al., 2008).

The scatter plot of ET and the energy partition given by the Bowen ratio ($\beta = H/\mathrm{LE}$) versus LAI is exhibited in Fig. 9, where more than 77% of the observed ET and β variation was explained by LAI (see Giambelluca et al., 2009). The dependency of ET on LAI as well as on the reference evapotranspiration was also reported for forests worldwide (Sun et al., 2011). The relationship between daily totals of ET normalized by the potential evaporation (Penman, 1948), versus the daily averages of g_c is presented in Fig. 10. The fitted equation was based on g_c bins and shows the physiological control of ET whose values approach the evaporative demand (Donohue et al., 2010) for g_c greater than 20 mm s^{-1}. Thus ET exhibits the effects of the canopy structure and physiology (Wallace and McJannet, 2010) as g_c is dependent on LAI, whose seasonal pattern co-varies with soil moisture and D (Hoffmann et al., 2005).
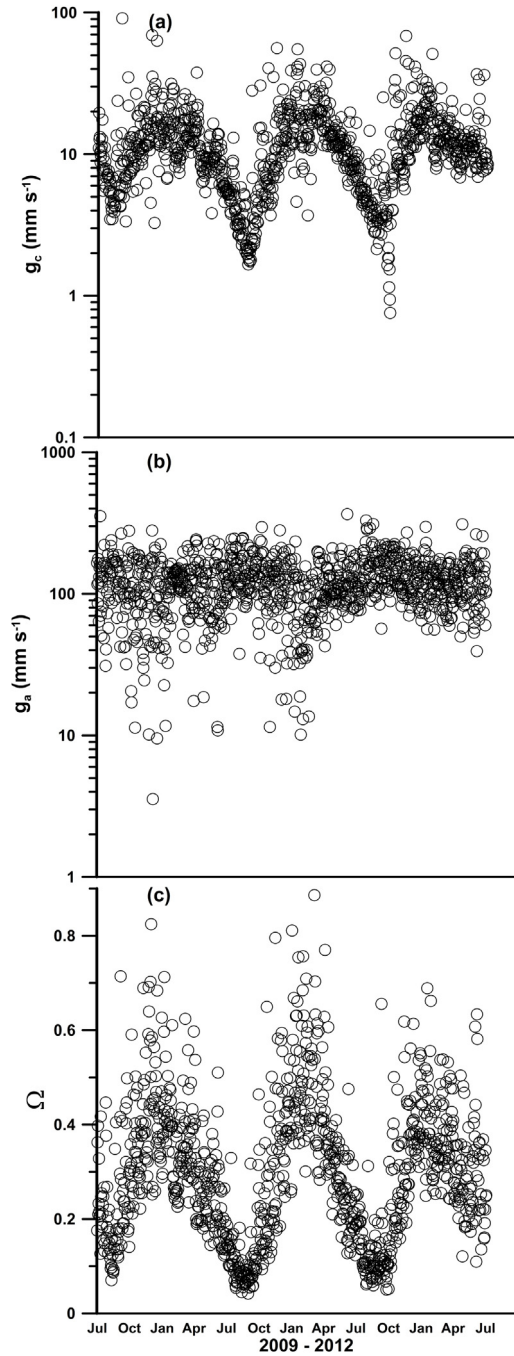
Fig. 6. Daily averages of: (a) canopy conductance (g_c); (b) aerodynamic conductance (g_a); (c) decoupling coefficient (Ω).
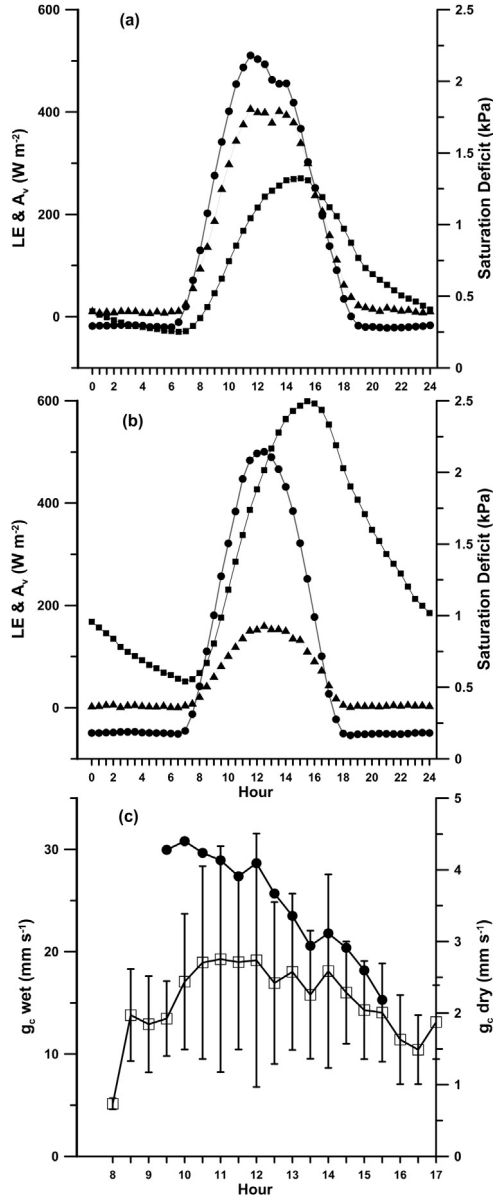
Fig. 7. Hourly averages of total evaporation (LE; triangles), available energy (A_v; circles) and saturation deficits (D; squares) in the rainy (a) and dry seasons (b). (c) Hourly averages of g_c in the rainy (squares) and dry (circles) seasons, the vertical bars represent the standard deviation of the means, only shown for the rainy-season.

To verify if there is a relationship between the bulk canopy conductance and the water vapor saturation deficit we selected g_c data when the PAR flux densities were above 1000 μmol quanta m^{-2} s^{-1}, minimizing the covariation with PAR and air temperature (Meinzer et al., 1999) and then divided g_c by LAI in order to reduce its seasonal influence on the estimated bulk canopy conductance (Eamus et al., 2001). The results are displayed in Fig. 11, where the g_c/LAI values represent the canopy conductance on a leaf area basis.
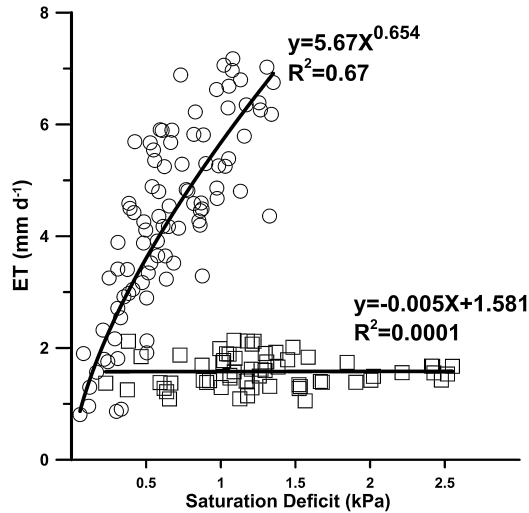
Fig. 8. Daily totals of evapotranspiration (ET) versus daily averages of water vapor saturation deficits (D) observed during the rainy-season (January–February–March; circles) and dry-season (July–August; gray squares). The best fit lines are also shown.
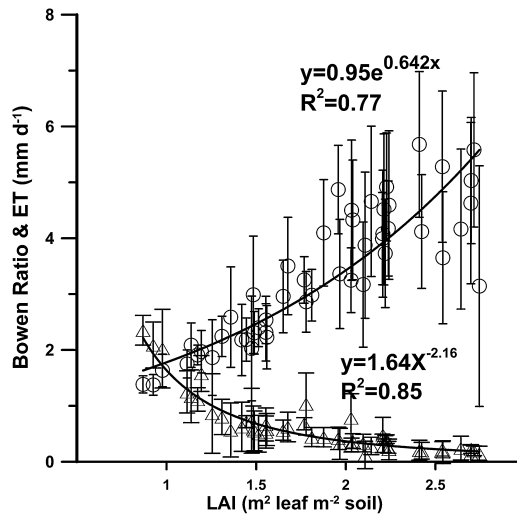

Fig. 9. Scatter plot of 15-day mean of daily evapotranspiration (ET, circles) and Bowen ratios (H/LE, triangles) versus the leaf area index (LAI) observed in the cerrado site. The equations displayed represent the fitted relationships and the vertical bars indicate the standard deviation of the mean.

The mean g_c/LAI calculated over D bins exhibited a strong exponential decrease following the increase in D as also observed by Bucci et al. (2005). However, despite the decrease in gas exchange surface in winter (see Goldstein et al., 2008) we did not observe higher canopy specific conductances (g_c/LAI). Therefore in this cerrado the atmospheric demand (A_v and D) mainly limited the evapotranspiration in the rainy-season and conversely in the dry-season ET was more limited by supply. However, the stronger physiological control can be advantageous when less water is available as it prevents the water potentials falling to dangerous levels promoting physiological dysfunction (see O'Grady et al., 2008; Goldstein et al., 2008).
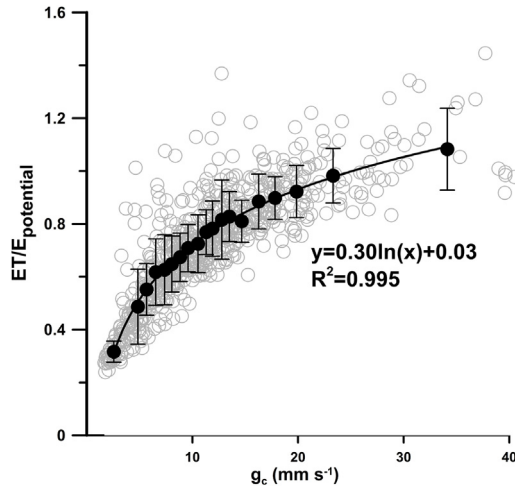
Fig. 10. Scatter plot of daily totals of evapotranspiration (ET) normalized by the potential evapotranspiration ($E_{potential}$) versus the canopy conductance (g_c). The fitted line was calculated for g_c bins (black circles) and the vertical bars represent the standard deviations.
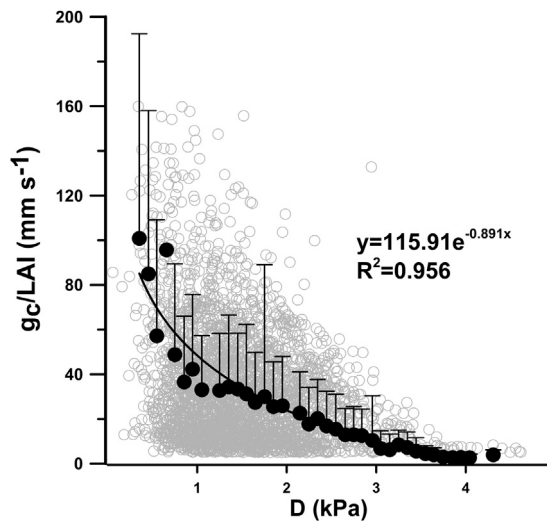

Fig. 11. Scatter plot of the bulk canopy conductance (g_c) normalized by the leaf area index (LAI) for PAR flux densities above 1000 μmol quanta m^{-2} s^{-1}. The fitted equation was calculated over humidity saturation deficit bins (D, black circles) and the vertical bars indicate +1 standard deviation.

4. Conclusions

Quantification of the actual evapotranspiration is a key issue for water management and it remains one of the most uncertain terms in the water balance globally (Miralles et al., 2011). For this *cerrado sensu-stricto* the mean evapotranspiration (1228 mm yr^{-1}) amounted to 82% of the long-term average rainfall (1498 mm yr^{-1}), thus accounting for a large proportion of the water budget. The mean evaporative fraction was 0.68; the interception accounted for 8% of rainfall, and the vegetation exhibited a strong surface control in parallel with the decrease in leaf area index, thus reducing the peak demand for water on a gradually declining store of soil water (Oishi et al., 2010) – evidence of adaptation to this seasonally dry climate (Hutley et al., 2000). Also, despite the 11% increase in the

annual rainfall observed in the wetter year, the water use increased only 4%, while the 16% decrease in rainfall observed in the third year did not affect ET, which shows the key role of cerrado on the supply of water to downstream areas.

The replacement of native vegetation by shallow-rooted crops, pasture and forestry will affect ecosystem physiognomy and phenology, rooting depth, surface and subsurface hydrology, and thus, energy partitioning. The characterization of the vegetation–atmosphere interactions obtained here can be used, with other savanna physiognomies, to verify the correctness of the modeling and remote sensing efforts (Pongratz et al., 2006; Christoffersen et al., 2014; Oliveira et al., 2014; da Silva et al., 2014) aimed at quantifying the impacts of land-use change on the regional surface energy and water balances (Han et al., 2012).

Conflicts of interest

There are no known conflicts of interest.

Acknowledgements

References

Aston, A.R., 1985. Heat storage in a young eucalypt forest. Agric. For. Meteorol. 35, 281–297.
Aubinet, M., Grelle, A., Ibrom, A., Rannik, U., Moncrieff, J., Foken, T., Kowalski, A.S., Martin, P.H., Berbigier, P., Bernhofer, Ch., Clement, R., Elbers, J., Granier, A., Grunwald, T., Morgenstern, K., Pilegaard, K., Rebmann, C., Snijders, W., Valentini, R., Vesala, T., 2000. Estimates of the annual net carbon and water exchange of forests: the EUROFLUX methodology. Adv. Ecol. Res. 30, 113–175.
Baldocchi, D., Falge, E., Gu, L., Olson, R., Hollinger, D., Running, S., Anthoni, P., Bernhofer, C., Davis, K., Evans, R., Fuentes, J., Goldstein, A., Katul, G., Law, B., Lee, X., Malhi, Y., Meyers, T., Munger, W., Oechel, W., Paw, U., Pilegaard, K.T., Schmid, K., Valentini, H.P., Verma, R., Vesala, S., Wilson, T., Wofsy, K.S., 2001. FLUXNET: a new tool to study the temporal and spatial variability of ecosystem-scale carbon dioxide, water vapor and energy flux densities. Bull. Am. Meteorol. Soc. 82, 2415–2434.
Baldocchi, D., 2003. Assessing the eddy covariance technique for evaluating carbon dioxide exchange rates of ecosystems: past, present and future. Global Change Biol. 9, 479–492.
Batalha, M.A., Mantovani, M., 2001. Floristic composition of the cerrado in the Pé-de-Gigante Reserve (Santa Rita do Passa Quatro, Southeastern Brazil). Acta Bot. Bras. 15, 289–304.
Batalha, M.A., Mantovani, W., de Mesquita Júnior, H.N., 2001. Vegetation structure in cerrado physiognomies in southeastern Brazil. Braz. J. Biol. 61, 475–483.
Batlle-Bayer, L., Batjes, N.H., Bindraban, P.S., 2010. Changes in organic carbon stocks upon land use conversion in the Brazilian Cerrado: a review. Agric. Ecosyst. Environ. 137, 47–58.
Bianchi, C.A., Haig, S.M., 2013. Deforestation trends of tropical dry forests in central Brazil. Biotropica 45, 395–400.
Biudes, M.S., Vourlitis, G.L., Machado, N.G., de Arruda, P.H.Z., Neves, G.A.R., Lobo, F.A., Neale, C.M.U., Nogueira, J.S., 2015. Patterns of energy exchange for tropical ecosystems across a climate gradient in Mato Grosso, Brazil. Agric. For. Meteorol. 202, 112–124.
Blanken, P.D., Black, T.A., 2004. The canopy conductance of a boreal aspen forest, Prince Albert National Park, Canada. Hydrol. Process. 18, 1561–1578.
Borgonovi, M., Chiarini, J.V., 1965. Cobertura vegetal do Estado de São Paulo I – Levantamento por fotointerpretação das áreas cobertas com Cerrado, Cerradão e Campo em 1965. Bragantia 24 (14), 160–172.
Borgonovi, M., Chiarini, J.V., do Amaral, A.Z., Coelho, A.G.S., Oliveira, D.A., 1967. Cobertura vegetal do Estado de São Paulo II – Levantamento por fotointerpretação das áreas cobertas com floresta natural e reflorestamento. Bragantia 26 (6), 93–102.
Brotzge, J.A., Duchon, C.E., 2000. A field comparison among a domeless net radiometer, two four-component net radiometers, and a domed net radiometer. J. Atmos. Ocean. Technol. 17, 1569–1582.
Bucci, S.J., Goldstein, G., Meinzer, F.C., Franco, A.C., Campanello, P., Scholz, F.G., 2005. Mechanisms contributing to seasonal homeostasis of minimum leaf water potential and predawn disequilibrium between soil and plant water potential in Neotropical savanna trees. Trees 19, 296–304.
Bucci, S.J., Scholz, F.G., Goldstein, G., Hoffmann, W.A., Meinzer, F.C., Franco, A.C., Giambelluca, T., Miralles-Wilhelm, F., 2008. Controls on stand transpiration and soil water utilization along a tree density gradient in a Neotropical savanna. Agric. For. Meteorol. 148, 839–849.

Burba, G.G., Mcdermitt, D.K., Grelle, A., Anderson, D.J., Xu, L.K., 2008. Addressing the influence of instrument surface heat exchange on the measurements of CO_2 flux from open-path gas analyzers. Global Change Biol. 14, 1854–1876.

Bustamante, M.M.C., Ferreira, L.G., 2011. Land use change and the carbon budget in the Brazilian Cerrado. In: Hill, M.J., Hanan, N.P. (Eds.), Ecosystem Function in Savannas: Measurement and Modeling at Landscape to Global Scales. CRC Press, pp. 367–381 (Chapter 19).

Cabral, O.M.R., Rocha, H.R., Gash, J.H.C., Ligo, M.A.V., Freitas, H.C., Tatsch, J.D., 2010. The energy and water balance of a Eucalyptus plantation in southeast Brazil. J. Hydrol. 388, 208–216.

Cabral, O.M.R., Rocha, H.R., Gash, J.H.C., Ligo, M.A.V., Tatsch, J.D., Freitas, H.C., Brasilio, E., 2012. Water use in a sugar-cane plantation. GCB Bioenergy 4, 555–565.

Canadell, J., Jackson, R.B., Ehleringer, J.R., Mooney, H.A., Sala, O.E., Schulze, E.-D., 1996. Maximum rooting depth of vegetation types at the global scale. Oecologia 108, 583–595.

Carlyle-Moses, D.E., 2004. Throughfall, stemflow, and canopy interception loss fluxes in a semi-arid Sierra Madre Oriental matorral community. J. Arid. Environ. 58, 181–202.

Christoffersen, B.O., Restrepo-Coupe, N., Arain, M.A., Baker, I.T., Cestaro, B.P., Ciais, P., Fisher, J.B., Galbraith, D., Guan, X., Gulden, L., van den Hurk, B., Ichii, K., Imbuzeiro, H., Jain, A., Levine, N., Miguez-Macho, G., Poulter, B., Roberti, D.R., Sakaguchi, K., Sahoo, A., Schaefer, K., Shi, M., Verbeeck, H., Yang, Z.-L., Araújo, A.C., Kruijt, B., Manzi, A.O., da Rocha, H.R., von Randow, C., Muza, M.N., Borak, J., Costa, M.H., de Gonçalves, L.G.G., Zeng, X., Saleska, S.R., 2014. Mechanisms of water supply and vegetation demand govern the seasonality and magnitude of evapotranspiration in Amazonia and Cerrado. Agric. For. Meteorol. 191, 33–50.

Czikowsky, M.J., Fitzjarrald, D.R., 2009. Detecting rainfall interception in an Amazonian rain forest with eddy flux measurements. J. Hydrol. 377, 92–105.

Culf, A.D., Foken, T., Gash, J.H.C., 2004. The energy balance closure problem. In: Kabat, P., Claussen, M., Dirmeyer, P.A., Gash, J.H.C., Bravo de Guenni, L., Meybeck, M., Pielke Sr., R.A., Vorosmarty, C.J., Hutjes, R.W.A., Lutkmeier, S. (Eds.), Vegetation, Water, Humans & The Climate. Springer-Verlag, Berlin, pp. 159–166, ISBN:3-540-42400-8.

da Rocha, H.R., Freitas, H.C., Rosolem, R., Juárez, R.I.N., Tannus, R.N., Ligo, M.A., Cabral, O.M.R., Dias, M.A.F.S., 2002. Measurements of CO_2 exchange over a woodland savanna (Cerrado sensu stricto) in southeast Brasil. Biota Neotrop. 2 (1), http://www.biotaneotropica.org.br/v2n1/pt/abstract?article+BN01702012002 (last accessed in 29.02.14).

da Rocha, H.R., Manzi, A.O., Cabral, O.M., Miller, S.D., Goulden, M.L., Saleska, S.R., Restrepo-Coupe, N., Wofsy, S.C., Borma, L.S., Artaxo, P., Vourlitis, G., Nogueira, J.S., Cardoso, F.L., Nobre, A.D., Kruijt, B., Freitas, H.C., von Randow, C., Aguiar, R.G., Maia, J.F., 2009. Patterns of water and heat flux across a biome gradient from tropical forest to savanna in Brazil. J. Geophys. Res. G: Biogeosci. 114, G00B12, http://dx.doi.org/10.1029/2007JG000640.

da Silva, B.B., Wilcox, B.P., da Silva, V.D.P.R., Montenegro, S.M.G.L., de Oliveira, L.M.M., 2014. Changes to the energy budget and evapotranspiration following conversion of tropical savannas to agricultural lands in Sao Paulo State, Brazil. Ecohydrology, http://dx.doi.org/10.1002/eco.1580.

David, T.S., Gash, J.H.C., Valente, F., Pereira, J.S., Ferreira, M.I., David, J.S., 2006. Rainfall interception by an isolated evergreen oak tree in a Mediterranean savannah. Hydrol. Process. 20, 2713–2726.

Domec, J.-C., Scholz, F.G., Bucci, S.J., Meinzer, F.C., Goldstein, G., Villalobos-Vega, R., 2006. Diurnal and seasonal variation in root xylem embolism in neotropical savanna woody species: impact on stomatal control of plant water status. Plant Cell Environ. 29, 26–35.

Donohue, R.J., McVicar, T.R., Roderick, M.L., 2010. Assessing the ability of potential evaporation formulations to capture the dynamics in evaporative demand within a changing climate. J. Hydrol. 386, 186–197.

Dufek, A.S., Ambrizzi, T., 2008. Precipitation variability in São Paulo State, Brazil. Theor. Appl. Climatol. 93, 167–178.

Eamus, D., Hutley, L.B., O'Grady, A.P., 2001. Daily and seasonal patterns of carbon and water fluxes above a north Australian savanna. Tree Physiol. 21, 977–988.

Falge, E., Baldocchi, D., Olson, R., Anthoni, P., Aubinet, M., Bernhofer, C., Burba, G., Ceulemans, R., Clement, R., Dolman, H., Granier, A., Gross, P., Grunwald, T., Hollinger, D., Jensen, N.O., Katul, G., Keronen, P., Kowalski, A., Lai, C.T., Law, B.E., Meyers, T., Moncrieff, J., Moors, E., Munger, J.W., Pilegaard, K., Rannik, U., Rebmann, C., Suyker, A., Tenhunen, J., Tu, K., Verma, S., Vesala, T., Wilson, K., Wofsy, S., 2001. Gap filling strategies for defensible annual sums of net ecosystem exchange. Agric. For. Meteorol. 107, 43–69.

Ferreira, J.N., Bustamente, M., Garcia-Montiel, D.C., Caylor, K.K., Davidson, E.A., 2007. Spatial variation in vegetation structure coupled to plant available water determined by two-dimensional soil resistivity profiling in a Brazilian savanna. Oecologia 153, 417–430.

Fidelis, A.T., Godoy, S.A.P., 2003. Estrutura de um cerrado stricto sensu na gleba cerrado Pé-de-Gigante, Santa Rita do Passa Quatro, SP. Acta Bot. Bras. 17, 531–539.

Foken, T., 2008. The energy balance closure problem – an overview. Ecol. Appl. 18, 1351–1367.

Frank, J.M., Massman, W.J., Ewers, B.E., 2013. Underestimates of sensible heat flux due to vertical velocity measurements errors in non-orthogonal sonic anemometers. Agric. For. Meteorol. 171–172, 72–81.

Frazer, G.W., Fournier, R.A., Trofymow, J.A., Hall, R.J., 2001. A comparison of digital and film fisheye photography for analysis of forest canopy structure and gap light transmission. Agric. For. Meteorol. 109, 249–263.

Gash, J.H.C., Wallace, J.S., Lloyd, C.R., Dolman, A.J., Sivakumar, M.V.K., Renard, C., 1991. Measurements of evaporation from fallow Sahelian savannah at the start of the dry season. Quart. J. R. Meteorol. Soc. 117, 749–760.

Gash, J.H.C., Lloyd, C.R., Lachaud, G., 1995. Estimating sparse forest rainfall interception with an analytical model. J. Hydrol. 170, 79–86.

Gash, J.H.C., Kabat, P., Monteny, B.A., Amadou, M., Bessemoulin, P., Billing, H., Blyth, E.M., DeBruin, H.A.R., Elbers, J.A., Friborg, T., 1997. The variability of evaporation during the HAPEX-Sahel Intensive Observation Period. J. Hydrol. 188, 385–399.

Gash, J.H.C., Valente, F., David, J.S., 1999. Estimates and measurements of evaporation from wet, sparse pine forest in Portugal. Agric. For. Meteorol. 94, 149–158.

Giambelluca, T.W., Scholz, F.G., Bucci, S.J., Meinzer, F.C., Goldstein, G., Hoffmann, W.A., Franco, A.C., Buchert, M.P., 2009. Evapotranspiration and energy balance of Brazilian savannas with contrasting tree density. Agric. For. Meteorol. 149, 1365–1376.

Goldstein, G., Meinzer, F.C., Bucci, S.J., Scholz, F.G., Franco, A.C., Hoffmann, W.A., 2008. Water economy of Neotropical savanna trees: six paradigms revisited. Tree Physiol. 28, 395–404.

Goulart, M.F., Lemos Filho, J.P., Lovato, M.B., 2005. Phenological variation within and among populations of Plathymenia reticulata in Brazilian Cerrado, the Atlantic forest and transitional sites. Ann. Bot. 96, 445–455.

Grace, J., San José, J., Meir, P., Miranda, H.S., Montes, R.A., 2006. Productivity and carbon fluxes of tropical savannas. J. Biogeogr. 33, 387–400.

Han, S., Xu, D., Wang, S., 2012. Decreasing potential evaporation trends in China from 1956 to 2005: accelerated in regions with significant agricultural influence? Agric. For. Meteorol. 154–155, 44–56.

Hoffmann, W.A., da Silva Jr., E.R., Machado, G.C., Bucci, S.J., Scholz, F.G., Goldstein, G., Meinzer, F.C., 2005. Seasonal leaf dynamics across a tree density gradient in a Brazilian savanna. Oecologia 145, 307–316.

Horst, T.W., Lenschow, H.D., 2009. Attenuation of scalar fluxes measured with spatially-displaced sensors. Boundary-Layer Meteorol. 130, 275–300.

Hsieh, C.I., Katul, G., Chi, T., 2000. An approximate analytical model for footprint estimation of scaler fluxes in thermally stratified atmospheric flows. Adv. Water Resour. 23, 765–772.

Hutley, L.B., O'Grady, A.P., Eamus, D., 2000. Evapotranspiration from Eucalypt open-forest savanna of Northern Australia. Funct. Ecol. 14, 183–194.

Ibrom, A., Dellwik, E., Flyvbjerg, H., Jensen, N.O., Pilegaard, K., 2007. Strong low-pass filtering effects on water vapor flux measurements with closed path eddy correlation systems. Agric. For. Meteorol. 147, 140–156.

Jarvis, P.G., 1985. Coupling of transpiration to the atmosphere in horticultural crops: the omega factor. Acta Hortic. 171, 187–205.

Kaimal, J.C., Finnigan, J.J., 1994. Atmospheric Boundary Layer Flows: their Structure and Measurement. Oxford University Press, Oxford, pp. 289.

Kirschbaum, M.U.F., Keith, H., Leuning, R., Cleugh, H.A., Jacobsen, K.L., van Gorsel, E., Raison, R.J., 2007. Modelling net ecosystem carbon and water exchange of a temperate Eucalyptus delegatensis forest using multiple constraints. Agric. For. Meteorol. 145, 48–68.

Klink, C.A., Machado, R.B., 2005. Conservation of the Brazilian Cerrado. Conserv. Biol. 19, 707–713.

Kutsch, W.L., Hanan, N., Scholes, B., McHugh, I., Kubheka, W., Eckardt, H., Williams, C., 2008. Response of carbon fluxes to water relations in a savanna ecosystem in South Africa. Biogeosciences 5, 1797–1808.

Lenza, E., Klink, C.A., 2006. Comportamento fenológico de espécies lenhosas em um cerrado sentido restrito de Brasília, DF. Rev. Bras. Bot. 29 (4), 627–638.

Leuning, R., Cleugh, H., Zegelin, S., Hughes, D., 2005. Carbon and water fluxes over a temperate Eucalyptus forest and tropical wet/dry savanna in Australia. Agric. For. Meteorol. 129, 151–173.

Lloyd, C.R., Gash, J.H.C., Shuttleworth, W.J., 1988. The measurement and modelling of rainfall interception by Amazonian rainforest. Agric. For. Meteorol. 43, 277–294.

Lloyd, J., Goulden, M.L., Ometto, J.P., Patiño, S., Fyllas, N.M., Quesada, C.A., 2009. Ecophysiology of forest and savanna vegetation. In: Keller, M., Bustamante, M., Gash, J., Silva Dias, P. (Eds.), Amazonia and Global Change. American Geophysical Union, Washington, DC, pp. 463–484.

Lilienfein, J., Wilcke, W., 2004. Water and element input into native, agri- and silvicultural ecosystems of the Brazilian savanna. Biogeochemistry 67, 183–212.

Lorz, C., Abbt-Braun, G., Bakker, F., Borges, P., Börnick, H., Fortes, L., Frimmel, F.H., Gaffron, A., Hebben, N., Höfer, R., Makeschin, F., Neder, K., Roig, L.H., Steiniger, B., Strauch, M., Walde, D., Weiß, H., Worch, E., Wummel, J., 2012. Challenges of an integrated water resource management for the Distrito Federal, Western Central Brazil: climate, land-use and water resources. Environ. Earth Sci. 65, 1575–1586.

Marengo, J.A., Camargo, C.C., 2008. Surface air temperature trends in Southern Brazil for 1960–2002. Int. J. Climatol. 28, 893–904.

Marris, E., 2005. Conservation in Brazil: the forgotten ecosystem. Nature 437, 944–945.

McNaughton, K.G., Jarvis, P.G., 1983. Predicting effects of vegetation changes on transpiration and evaporation. In: Kozlowski, T.T. (Ed.), Water Deficits and Plant Growth, vol. 7. Academic Press, New York, pp. 1–47.

Meinzer, F.C., Goldstein, G., Franco, A.C., Bustamante, M., Igler, E., Jackson, P., Caldas, L., Rundel, P.W., 1999. Atmospheric and hydraulic limitations on transpiration in Brazilian cerrado woody species. Funct. Ecol. 13, 273–282.

Michiles, A.A.S., Gielow, R., 2008. Above-ground thermal energy storage rates, trunk heat fluxes and surface energy balance in a central Amazonian rainforest. Agric. For. Meteorol. 148, 917–930.

Miralles, D.G., De Jeu, R.A.M., Gash, J.H., Holmes, T.R.H., Dolman, A.J., 2011. Magnitude and variability of land evaporation and its components at the global scale. Hydrol. Earth Syst. Sci. 15, 967–981.

Miranda, A.C., Miranda, H.S., Lloyd, J., Grace, J., Francey, R.J., McIntyre, J.A., Meir, P., Riggan, P., Lockwood, R., Brass, J., 1997. Fluxes of carbon, water and energy over Brazilian cerrado: an analysis using eddy covariance and stable isotopes. Plant Cell Environ. 20, 315–328.

Myers, N., Mittermeier, R.A., Mittermeier, C.G., da Fonseca, G.A.B., Kent, J., 2000. Biodiversity hotspots for conservation priorities. Nature 403, 853–858.

Monteith, J.L., 1965. Evaporation and environment. In: The State and Movement of Water in Living Organisms. Proc. 19th Symp. Soc. Exp. Biol., Swansea 1964. Cambridge University Press, Cambridge, pp. 205–234.

Moore, C.J., Fisch, G.F., 1986. Estimating heat storage in Amazonian tropical forest. Agric. For. Meteorol. 38, 147–169.

O'Grady, A.P., Worledge, D., Battaglia, M., 2008. Constraints on transpiration of Eucalyptus globules in southern Tasmania, Australia. Agric. For. Meteorol. 148, 453–465.

Oishi, A.C., Oren, R., Novick, K.A., Palmroth, S., Katul, G.G., 2010. Interannual invariability of forest evapotranspiration and its consequence to water flow downstream. Ecosystems, http://dx.doi.org/10.1007/s10021-010-9328-3.

Oliphant, A.J., Grimmond, C.S.B., Zutter, H.N., Schmid, H.P., Su, H.-B., Scott, S.L., Offerle, B., Randolph, J.C., Ehman, J., 2004. Heat storage and energy balance fluxes for a temperate deciduous forest. Agric. For. Meteorol. 126, 185–201.

Oliveira, P.T.S., Nearing, M.A., Moran, M.S., Goodrich, D.C., Wendland, E., Gupta, H.V., 2014. Trends in water balance components across the Brazilian Cerrado. Water Resour. Res. 50, 7100–7114, http://dx.doi.org/10.1002/2013WR015202.

Oliveira, R.S., Bezerra, L., Davidson, E.A., Pinto, F., Klink, C.A., Nepstad, D.C., Moreira, A., 2005. Deep root function in soil water dynamics in cerrado savannas of central Brazil. Funct. Ecol. 19, 574–581.

Penman, H.L., 1948. Natural evaporation from open water, bare soil and grass. Proc. Roy. Soc. Lond., Ser. A 193, 120–145.

Pereira, F.L., Gash, J.H.C., David, J.S., David, T.S., Monteiro, P.R., Valente, F., 2009. Modelling interception loss from evergreen oak Mediterranean savannas: application of a tree-based modelling approach. Agric. For. Meteorol. 149, 680–688.

Pongratz, J., Bounoua, L., DeFries, R.S., Morton, D.C., Anderson, L.O., Mauser, W., Klink, C.A., 2006. The impact of land cover change on surface energy and water balance in Mato Grosso, Brazil. Earth Interact. 10 (19), 1–17.

Quesada, C.A., Miranda, A.C., Hodnett, M.G., Santos, A.J.B., Miranda, H.S., Breyer, L.M., 2004. Seasonal and depth variation of soil moisture in a burned open savanna (campo sujo) in central Brazil. Ecol. Appl. 14, S33–S41.

Quesada, C.A., Hodnett, M.G., Breyer, L.M., Santos, A.J.B., Andrade, S., Miranda, H.S., Miranda, A.C., Lloyd, J., 2008. Seasonal variations in soil water in two woodland savannas of central Brazil with different fire history. Tree Phys. 28, 405–415.

Quirino, W.F., Vale, A.T., Andrade, A.P.A., Abreu, L.S., Azevedo, A.C.S., 2005. Poder calorífico da madeira e de materiais ligno-celulósicos. Rev. Madeira 89, 100–106.

Rezende, A.V., Vale, A.T., Sanquetta, C.R., Figueiredo Filho, A., Felfili, J.M., 2006. Comparação de modelos matemáticos para estimativa do volume, biomassa e estoque de carbono da vegetação lenhosa de um cerrado sensu stricto em Brasília, DF. Sci. For. 71, 65–76.

Roberts, J., Cabral, O.M.R., Fisch, G., Molion, L.C.B., Moore, C.J., Shuttleworth, W.J., 1993. Transpiration from an Amazonian rainforest calculated from stomatal conductance measurements. Agric. For. Meteorol. 65, 175–196.

Rodrigues, T.R., Vourlitis, G.L., Lobo, F.D.A., de Oliveira, R.G., Nogueira, J.D.S., 2014. Seasonal variation in energy balance and canopy conductance for a tropical savanna ecosystem of south central Mato Grosso, Brazil. J. Geophys. Res. Biogeosci. 119, http://dx.doi.org/10.1002/2013JG002472.

Ruggiero, P.G.C., Batalha, M.A., Pivello, V.R., Meirelles, S.T., 2002. Soil-vegetation relationships in cerrado (Brazilian savanna) and semideciduous forest, Southeastern Brazil. Plant Ecol. 160, 1–16.

San Jose, J.J., Montes, R., 1992. Rainfall partitioning by semideciduous forest grove in the savannas of the Orinoco Llanos, Venezuela. J. Hydrol. 132, 249–262.

Sakai, R.K., Fitzjarrald, D.R., Moore, K.E., 2001. Importance of low-frequency contributions to eddy fluxes observed over rough surfaces. J. Appl. Meteorol. 40, 2178–2192.

Santos, A.J.B., Silva, G.T.D.A., Miranda, H.S., Miranda, A.C., Lloyd, J., 2003. Effects of fire on surface carbon, energy and water vapour fluxes over campo sujo savanna in central Brazil. Funct. Ecol. 17, 711–719.

Schmid, H.P., 1997. Experimental design for flux measurements: matching scales of observations and fluxes. Agric. For. Meteorol. 87, 179–200.

Schmid, H.P., Lloyd, C.R., 1999. Spatial representativeness and the location bias of flux footprints over inhomogeneous areas. Agric. For. Meteorol. 93, 195–209.

SEMA, 2005. Inventário florestal da vegetação natural do Estado de São Paulo. São Paulo, Secretaria do Meio Ambiente. Instituto Florestal, Imprensa Oficial – SP, pp. 200.

Silberstein, R., Held, A., Hatton, T., Viney, N., Sivapalan, M., 2001. Energy balance of a natural Jarrah (*Eucalyptus marginata*) forest in Western Australia: measurements during the spring and summer. Agric. For. Meteorol. 109, 79–104.

Silva, J.F., Fariñas, M.R., Felfili, J.M., Klink, C.A., 2006. Spatial heterogeneity, land use and conservation in the cerrado region of Brazil. J. Biogeogr. 33, 536–548.

Šimůnek, J., van Genuchten, M.T., Šejna, M., 2008. Development and applications of the HYDRUS and STANMOD software packages and related codes. Vadose Zone J. 7, 587–600.

Su, H., Schmid, H., Grimmond, S., Vogel, C., Oliphant, A., 2004. Spectral characteristics and correction of long-term eddy-covariance measurements over two mixed hardwood forests in non-flat terrain. Boundary-Layer Meteorol. 110, 213–253.

Sun, G., Alstad, K., Chen, J., Chen, S., Ford, C.R., Lin, G., Liu, C., Lu, N., McNulty, S.G., Miao, H., Noormets, A., Vose, J.M., Wilske, B., Zeppel, M., Zhang, Y., Zhang, Z., 2011. A general predictive model for estimating monthly ecosystem evapotranspiration. Ecohydrology 4, 245–255.

Valente, F., David, J.S., Gash, J.H.C., 1997. Modelling interception loss for two sparse eucalypt and pine forests in central Portugal using reformulated Rutter and Gash analytical models. J. Hydrol. 190, 141–162.

Valenti, M.W., Cianciaruso, M.V., Batalha, M.A., 2008. Seasonality of litterfall and leaf decomposition in a cerrado site. Braz. J. Biol. 68, 459–465.

Vourlitis, G.L., Nogueira, J.S., Lobo, F.A., Sendall, K.M., de Paulo, S.R., Dias, C.A.A., Pinto Jr., O.B., de Andrade, N.L.R., 2008. Energy balance and canopy conductance of a tropical semi-deciduous forest of the southern Amazon Basin. Water Resour. Res. 44, W03412, http://dx.doi.org/10.1029/2006WR005526.

Vourlitis, G.L., da Rocha, H.R., 2011. Flux dynamics in the Cerrado and Cerrado–Forest transition. In: Hill, M.J., Hanan, N.P. (Eds.), Ecosystem Function in Savannas: Measurement and Modeling at Landscape to Global Scales. CRC Press, pp. 97–116 (Chapter 5).

Vourlitis, G.L., Nogueira, J.S., Lobo, F.A., Pinto Jr., O.B., 2014. Variations in evapotranspiration and climate for an Amazonian semi-deciduous forest over seasonal, annual, and El Niño cycles. Int. J. Biometeorol., http://dx.doi.org/10.1007/s00484-014-0837-1.

Wallace, J., McJannet, D., 2008. Modelling interception in coastal and montane rainforests in northern Queensland, Australia. J. Hydrol. 348, 480–495.

Wallace, J., McJannet, D., 2010. Processes controlling transpiration in the rainforests of north Queensland, Australia. J. Hydrol. 384, 107–117.

Webb, E.K., Pearman, G.I., Leuning, R.G., 1980. Correction of flux measurements for density effects due to heat and water vapour transfer. Quart. J. R. Meteorol. Soc. 106, 85–100.

Williams, R.J., Myers, B.A., Muller, W.J., Duff, G.A., Eamus, D., 1997. Leaf phenology of woody species in a north Australian tropical savanna. Ecology 78, 2542–2558.

Wilson, K.B., Hanson, P.J., Mulholland, P.J., Baldocchi, D.D., Wullschleger, S.D., 2001. A comparison of methods for determining forest evapotranspiration and its components: sap-flow, soil water budget, eddy covariance and catchment water balance. Agric. For. Meteorol. 106, 153–168.

Zeppel, M.J.B., Macinnis-Ng, C.M.O., Yunusa, I.A.M., Whitley, R.J., Eamus, D., 2008. Long term trends of stand transpiration in a remnant forest during wet and dryyears. J. Hydrol. 349, 200–213.